Research Article | Vol. 29, No. 23 / 8 Nov 2021 / Optics Express 38849
Optics EXPRESS

Observation of optical vortex knots and links associated with topological charge

JINZHAN ZHONG,[1] SHENG LIU,[1,2] XUYUE GUO,[1] PENG LI,[1] BINGYAN WEI,[1] LEI HAN,[1] SHUXIA QI,[1] AND JIANLIN ZHAO[1,3]

[1] *Key Laboratory of Light Field Manipulation and Information Acquisition, Ministry of Industry and Information Technology, and Shaanxi Key Laboratory of Optical Information Technology, School of Physical Science and Technology, Northwestern Polytechnical University, Xi'an 710129, China*
[2] *shengliu@nwpu.edu.cn*
[3] *jlzhao@nwpu.edu.cn*

Abstract: Knots and links, as three-dimensional topologies, have played a fundamental role in many physical fields. Despite knotted vortex loops having been shown to exist in the light field, the three-dimensional configuration of vortex loop is fixed due to their topological robustness, making the fields with different topologies independent of each other. In this work, we established the mapping between the torus knots/links and the integer topological charge of the optical vortex, and demonstrated the change of the intermediate state with fractional charges. Furthermore, we experimentally observed the transformation process of the three-dimensional topological structure by only changing the topological charge. Remarkably, we revealed two different reconnection mechanisms associated with the odd or even index of the torus topology. We hope these results may provide new insight for the study of singular optics and evolution in other physical fields.

1. Introduction

In recent years, as topologically stable objects, knots and links have been shown to play an important role in a wide range of physical fields [1–5]. The static knotted structures have been studied in liquid crystals and Bose-Einstein condensates [6–8], and the physical process of knotting has gradually become a bridge between classical and quantum field theories [9]. In optical systems, the three-dimensional (3D) configuration of topologies mainly combines concepts related to singular optics [10–12], which has gradually become a new branch of modern optics [13]. Among them, the vortex beam with orbital angular momentum (OAM) is widely concerned [14]. Such a single singularity beam naturally forms an axial vortex line in free space or linear medium, but knotted or linked vortex loops are surprisingly found in the light speckle field with complex tangled vortex line [15]. Dedicated to generate the optical vortex field with topological structure artificially, a lot of theoretical and experimental studies have been carried out [16–23]. Accordingly, similar torus topologies can be embedded in the longitudinal polarization components of light and created as polarization singularity lines [24–27]. The latter can be considered as information carrier due to the rich topology invariant [28]. More importantly, it is possible to produce light beams with knotted trajectories of high intensity and phase gradients for particle manipulation [29]. Beyond the monochromatic light field, the knotted trajectories can be produced taking advantage of the polychromatic light [30,31].

Till now, the reported optical vortex knots and links are fixed due to the topological robustness [18,19]. Although the topology carrying beams exhibit the expected topological properties, the differences in topological structures cause that the fields can only be created independently. Therefore, it is important to clarify the relationship between a series of optical vortex knots and links and further to generate the related optical vortex torus topologies. Topologically, the knots and links are not homeomorphic and thus cannot transform into each other naturally [32]. In other words, the transformation of a knot (single loop) into a link (two loops) requires the necessary

#441263 https://doi.org/10.1364/OE.441263
Journal © 2021 Received 23 Aug 2021; revised 9 Oct 2021; accepted 28 Oct 2021; published 5 Nov 2021

Optics EXPRESS

structural changes, which need to be driven artificially. However, it is not clear whether there are intermediate states between optical vortex knots and vortex links. Considering this problem brings to mind the interesting evolution of fractional vortices between integer vortices [33]. Fractional optical vortices show unexpected properties in definition [34–36], angular momentum state and practical application [37–39]. Therefore, it is necessary to consider the effect of phase step caused by fractional vortices on the 3D topology.

In this paper, we theoretically established the mapping between the torus knots/links and the integer topological charge of the optical vortex, and showed that fractional vortex is the key to establish the intermediate state between optical vortex knots and vortex links. We experimentally generated a series of related optical vortex torus topologies, and furthermore, observed the evolution process of the 3D topological structure of light field. The results well demonstrated the transformation process between optical vortex knots and links only by changing the topological charge. Remarkably, we revealed two different reconnection processes associated with the odd and even indices of the torus topology. The present work is expected to provide ideas for the topological diversity of vortex light field and offer a glimpse into the evolution of singular light field.

2. Theoretical model

A relatively simple class of knots are the torus knots, which can be considered as a closed thread enwind around a torus surface. Thanks to the topological invariance, the closed curve can be spatially deformed and homeomorphic with its braided representation [40]. For instance, the plane diagram of the Trefoil knot shown in Fig. 1(a) represents the geometrical relationship at each crossing, which can also be reflected in the braided representation shown in Fig. 1(b). The formation of an optical vortex knot in 3D space benefits from the inverse process of the conceptual demonstration, which can be realized by a stereographic projection [41,42]. In this case, the periodic braids [Fig. 1(d)] are the zeros of a function of u as a variable in complex space

$$p_h^n(u) = \prod_{j=1}^{2} (u - s_j(nh)), \tag{1}$$

where h denotes the height coordinate of the braided zeros, and the range of the variable is $[0, \pi]$. The periodic trigonometrical function satisfies relationship $s_j(h+2\pi) = s_j(h)$, (j=1,2 numbers the zeroes). The parameter n is denoted as the repetitions of the basic braid crossing structure (the section marked with the arrow in Fig. 1(d, f)). Replacing $s_j(nh)$ with the exponential function, $v=(-1)^{j-1}\exp(inh)$, Eq. (1) is then simplified to a complex polynomial with the coordinates (u, v)

$$q(u, v) = u^2 - v^n. \tag{2}$$

Then the constructed braided field can be converted into its corresponding topology in 3D real space with a stereographic projection defined by

$$u = \frac{R^2 + z^2 - 1 + 2iz}{R^2 + z^2 + 1}, \; v = \frac{2Re^{i\varphi}}{R^2 + z^2 + 1} \tag{3}$$

where (R, φ, z) are the cylindrical coordinates. Intuitively, this projection performs the task of docking the ends of the braided structure and maps the height coordinate h to the angular coordinate φ. The Trefoil knot embedded in 3D space for n=3 is shown in Fig. 1(c), correspondingly, the example of torus link when n is even as shown in Fig. 1(e).

To create optical vortex knots experimentally, one way is to combine Laguerre-Gauss (LG) beams under the paraxial propagation condition, which is a set of complete orthogonal bases [19,43]. In this case, the paraxial polynomial solutions at z=0 plane can be represented as the

Optics EXPRESS

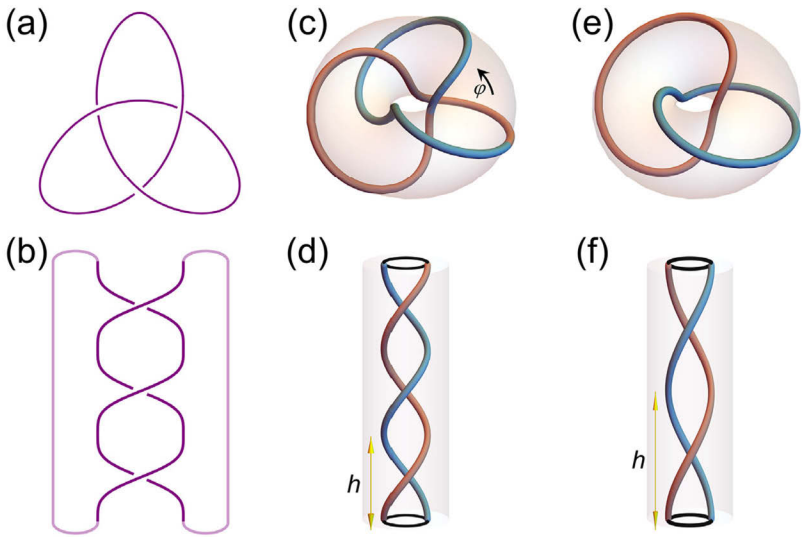

Fig. 1. Torus knots and its braid representation. (a) Schematic diagram of a Trefoil knot. (b) Braid representation of a Trefoil knot. (c) A Trefoil knot embedded in 3D real space obtained from the space projection of the periodic 2-strand braided zeros in (d). (e) A Hopf link embedded in 3D real space obtained from the space projection of the periodic 2-strand braided zeros in (f). The height ranges from 0 to π is indicated by the arrow in (d, f).

linear superposition of LG modes using Fourier-like integral [44]. From the source of the vortex, it can be divided into two components with non-zero and zero OAM, i.e.

$$\Psi(n, w_n) = \alpha_n \mathrm{LG}_n^0(w_n) + \sum_{p=0}^{n} \beta_n^p \mathrm{LG}_0^p(w_n), \tag{4}$$

where α_n, β_n^p are the coefficient weighting of each component, n is the topological charge, p is the radial index, and w_n is the beam waist. Consider the integer value n that is applied to the above model, the weight coefficients are completely different for different n. In addition, the number of LG modes with zero OAM is also different [19]. The fact that topological structures are non-homeomorphic and therefore the corresponding vortex light fields are constructed independently makes these differences naturally acceptable. Here, we prefer to obtain a series of related vortex light fields with torus topologies.

In essence, multiple stable vortices evolve in free space, which are often associated with higher order vortices, and the resulting 3D vortex lines intertwine to form a knotted trajectory. Notice from Eq. (4) that the vortex component LG_n^0 provides all the vortices that make up the vortex topology. Therefore, the parameter n determines not only the topology $T(2, n)$, but also the vortex component of the corresponding light field, which establishes a one-to-one mapping between the torus topology and the vortex phase. Another important element is the perturbation component consisting of multiple LG modes with zero OAM, which forms a phase step ring of π. For a larger index n, the superposition of more modes forms a phase ring with a larger inner diameter, which is a favorable condition for higher-order vortices. We find that the perturbation component with high index n can also act on low-order vortices. It means that it is possible to create a series of optical vortex torus topologies with the same perturbation component. Another important parameter of an optical vortex torus knot is the beam waist w_n of the LG mode components, which is significantly different for different topologies. Here, after the perturbation component is selected, we select the corresponding beam waist for all mode superposition components. For

Optics EXPRESS

example, if we use the perturbation component of $\Psi(5, w_5)$ [19], the modified vortex knot field with integer index n<6 can be expressed as

$$\begin{aligned}\Psi(n, 0.93) = {} & 0.061\mathrm{LG}_0^0 - 0.256\mathrm{LG}_0^1 + 0.615\mathrm{LG}_0^2 \\ & - 0.635\mathrm{LG}_0^3 + 0.292\mathrm{LG}_0^4 - 0.061\mathrm{LG}_0^5 - 0.245\mathrm{LG}_n^0.\end{aligned} \tag{5}$$

3. Experiment result

3.1. Generation of optical vortex knots/links with integer indices

Based on the above analysis, we experimentally generated and observed a series of related optical vortex torus topologies according to Eq. (5). Figure 2(a) shows the experimental setup for generating knot topologies. To observe the topological structure in a 3D light field, the resulting light field needs to meet the expected amplitude and phase distribution [Fig. 2($b_{1,2}$) as an example]. The phase-only pattern loaded on the SLM is shown in Fig. 2(b_3). The modulated beam is imaged by a 4f system and spatially filtered at the focal plane to obtain the required

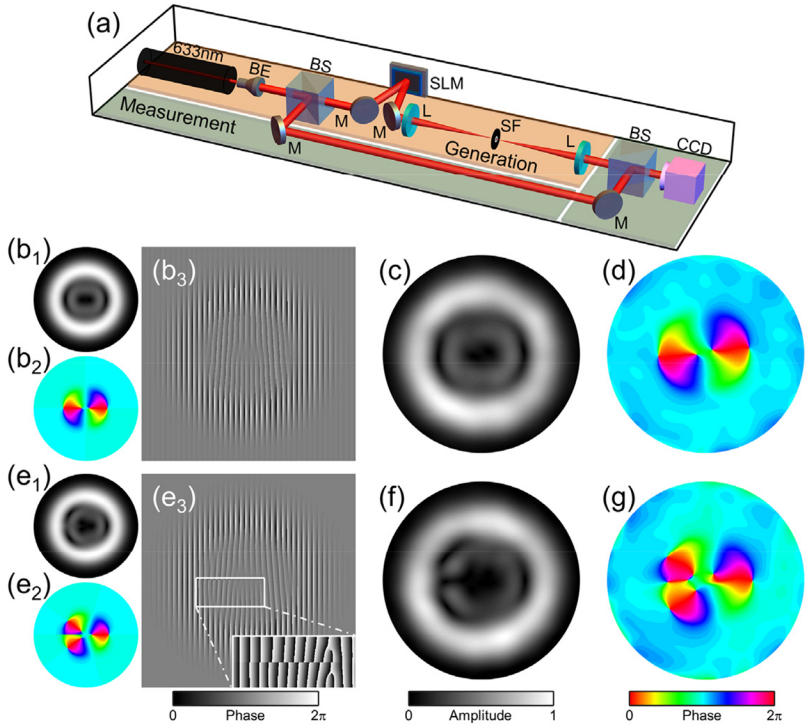

Fig. 2. Experimental generation of optical vortex torus knots. (a) Experimental setup used to generate and measurement optical vortex knots. The horizontally polarized light (He-Ne laser, 632.8 nm) is expanded by a beam expander (BE) as the input beam and divided into two beams through a beam splitter (BS): the reflected one is modulated by an addressed phase pattern loaded in a phase-type spatial light modulator (SLM), forming the vortex knot fields, while the transmitted one is used as the reference beam for interference. (b_1), (b_2) Amplitude and phase distributions of a Hopf link at the z=0 plane. (b_3) Phase pattern for generating optical vortex Hopf link. (c), (d) Measured amplitude and phase distributions of a Hopf link at the z=0 plane. (e_1), (e_2) Amplitude and phase distributions of the light field with the fractional index n=2.5 and (e_3) the phase pattern used in the experiment. (f), (g) Corresponding amplitude and phase distributions measured experimentally.

Optics EXPRESS

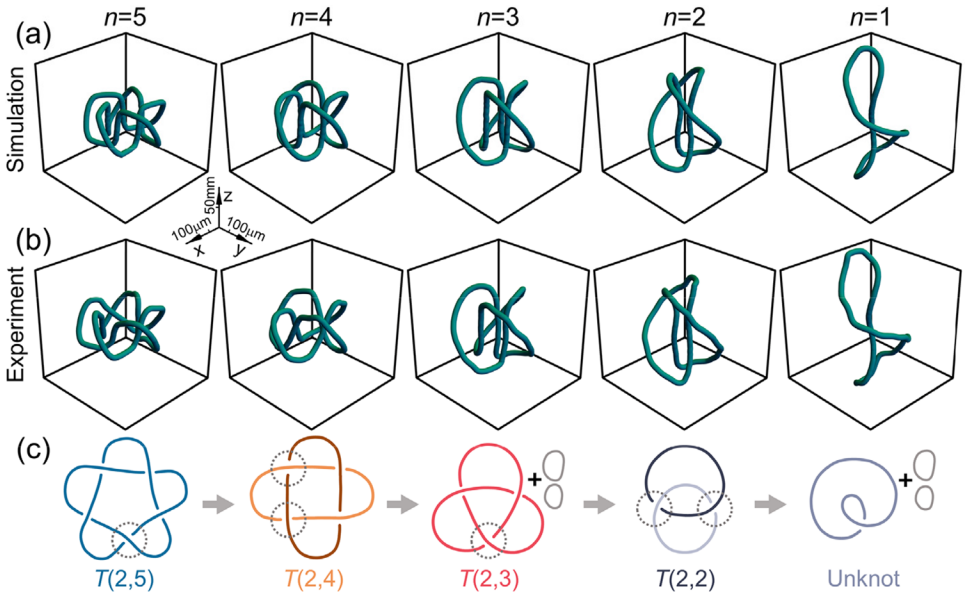

Fig. 3. Related optical vortex torus topologies. (a) Numerical and (b) experiment results of optical vortex knots (links) with different integer indices from n=5 to 1. (c) Schematic of reconnection (dissociation) event as n decreases. The dynamic processes are shown in Visualization 1 and Visualization 2.

first-order diffraction order, which is received by a charge coupled devices (CCD). By employing our method [23], the amplitude and phase distributions measured at the z=0 plane are shown in Fig. 2(c,d). By using SLM to control the phase distribution of vortex term, we generated and reconstructed the related optical vortex torus topologies with different integer indices from n=5 to 1, as shown in Fig. 3(b). The experiment results are consistent with the numerical simulation results shown in Fig. 3(a) and keep the corresponding topological characteristics. We have shown that Eq. (5) applies to all integers with n<6 experimentally. It demonstrates that a Cinquefoil knot (n=5), a Solomon link (n=4), a Trefoil knot (n=3), a Hopf link (n=2), and a single loop (n=1) are formed, respectively.

3.2. *Generation of optical vortex topologies with fractional indices*

Having built and experimentally generated the optical vortex torus topologies with integer indices, we now generalize them and consider the topologies generated by fractional vortices. For the fractional index n, the ends of the braided zero will not be in the same transverse position, so the stereographic projection of braid representation cannot form a closed structure. However, the linear superposition representation of light fields offers a possibility. Based on the conclusion in section 3.1, it is natural to consider fractional index for Eq. (5) further. Here we consider a vortex term consisting of a circularly symmetric amplitude distribution without discontinuity and a vortex phase distribution with fractional topological charge [38]. As an example, the amplitude and phase distributions of the light field with n=2.5 are shown in Figs. 2($e_{1,2}$). The dislocation of the grating due to phase discontinuity can be clearly seen from the inset in Fig. 2(e_3). Experimentally, we obtained continuous intensity and phase distributions, and the grating dislocation produced additional phase singularities, as shown in Fig. 2(g). In this case, the topological property of the light field is not destroyed by additional phase singularities. As one can see from Fig. 4(e), multiple vortices co-evolve to form a Hopf link in 3D space, although certain distortion occurs when compared with the case of n=2. In order to observe how a series of

Optics EXPRESS

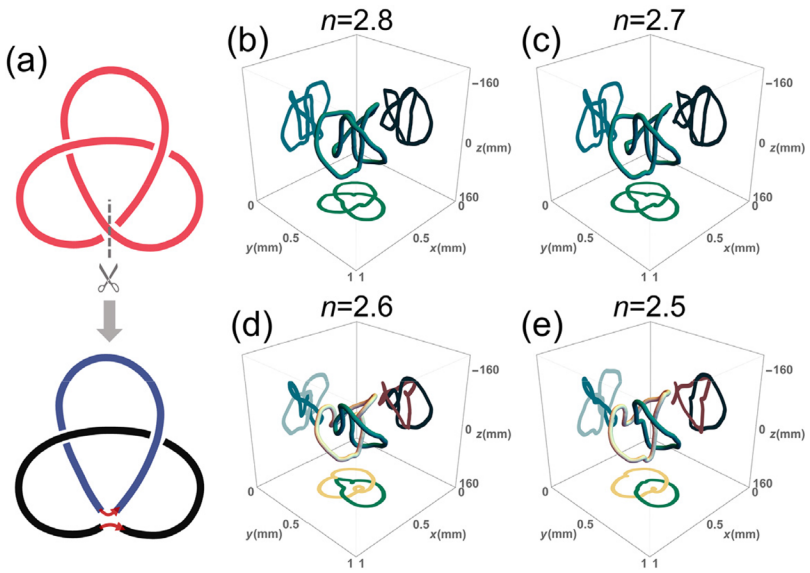

Fig. 4. Evolution of the field from odd index to even index. (a) Illustration of reconnection mechanism. (b-e) 3D topological structures observed experimentally for n=2.8, 2.7, 2.6, and 2.5, respectively. For convenience, individual optical vortex rings are represented in different colors.

related optical vortex torus topologies are transformed, we consider that the index n changes from 5 to 1 with an interval 0.1. The complete numerical simulation and experiment results are shown in Visualization 1 and Visualization 2, respectively. It can be seen that the topological structure changes from $T(2, 5)$ to $T(2, 1)$ during the dynamic process, accompanied by the reconnection of the vortex lines and even the dissociation and annihilation of additional loops. Illustration of this process is shown in Fig. 3(c). The areas where the reconnection happens are marked with the dotted circles. The local reconnection of the vortex line can shape the isolated optical vortex knot by cutting and splicing the nearby lines, like a pair of scissors.

4. Influence of fractional charges on the topological structure

We now discuss the physical mechanism of light field evolution as the index n decreases. In essence, the changes of vortex topology are caused by the interaction of multi-vortices embedded in the light field, associated with the intertwining, merging and annihilating of the vortex lines. It is notable that the adjacent vortex lines for reconnection always attract each other first till reconnect, and finally keep moving away. The evolution trend of the vortex lines is closely related to the phase distribution of the light field. Due to the addition of fractional vortices, the local reconnection of the vortex lines often occurs in the position of phase discontinuity. However, the evolution of the index n from odd to even is different from the evolution of even to odd, which we will discuss separately here.

The cases for the index n changing from odd to even (5→4 and 3→2) are readily comprehensible because the reconnection happens at one cross-string as shown in Fig. 4(a). One can imagine that the topological structure is split into two disconnected vortex lines but the original position relationship is maintained, then, the topology can be changed by simply closing these two independent vortices lines, the corresponding reconnections following the red arrows. Experimentally, we observed that this process occurred between n=2.7 and 2.6 as show in Figs. 4(b-e). The adjacent vortex lines were constantly closed and finally reconnected, resulting

Optics EXPRESS

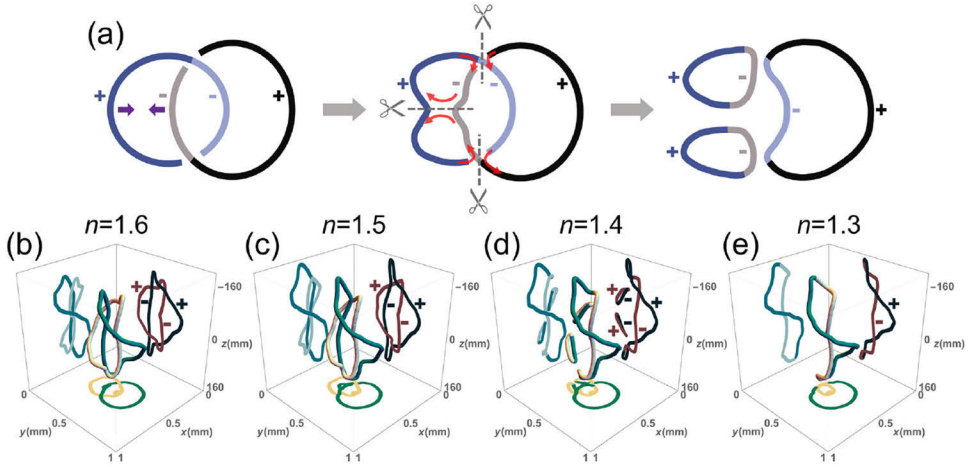

Fig. 5. Evolution of the field from even index to odd index. (a) Illustration of reconnection mechanism. (b-e) 3D topological structures observed experimentally for n=1.6, 1.5, 1.4, and 1.3, respectively. The different colors in (b, c) indicate different vortex loops. The different colors in (d, e) indicate the positive and negative topological charges.

in the transformation of a single closed vortex loop into two. This process can be better seen in a top view marked with different colors, representing different vortex loops. Accordingly, the position of the reconnection corresponds to the position of the phase discontinuity shown in Fig. 2(e_2).

For cases of the index n changing from even to odd (4→3 and 2→1), the reconnection is more complicated than previous case. Reconnection occurs at several cross-strings, accompanied by the generation of additional vortex loops. This process is determined by the topological properties of the structure and the properties of the optical vortex. To understand this process, we choose $T(2,2)\rightarrow T(2,1)$ as the illustration. Topologically, in order to make two closed loops form a single loop, cutting and splicing of two closed loops are necessary. In addition, the reconnection of the vortex lines needs to satisfy the propagation laws of the light field, which is crucial. The pair of vortices must have the opposite signs, so that they are allowed to merge with each other to form a closed loop during propagation. On above basis, Fig. 5(a) shows a planar schematic of the actual topology transformation process, where the vortex lines would be cut at the three positions marked by dashed lines and reconnected following the red arrows. Figures 5(b-e) show the experimentally observed topological structures corresponding to index n decreasing from 1.6 to 1.3. The plus and minus signs shown in the side view indicate the symbol of the corresponding vortex lines, which satisfies the reconnection rule. In addition, the generation of additional vortex rings is main caused by multiple reconnections, which leads to the change of the total number of independent vortex loops in 3D space directly. This parameter may facilitate the identification of topology transformation process. Eventually, when the index drops to 1, the vortex loop becomes unlinked and unknotted, despite the local distortion in space. As an outlook, the construction of more complex vortex topology and the corresponding topology transformation may benefit from polynomial Gaussian beams [45–47].

5. Conclusions

In conclusion, we separated complicated optical vortex torus topologies into combinations of more meaningful vortex term and perturbation term. Applying this model, we revealed the mapping relationship between the torus topology and vortex phase and obtained a series of

Optics EXPRESS

related optical vortex torus topologies experimentally. We further extended it to fractional vortices and showed a series of intermediate states of the transformation of optical vortex torus topologies. Moreover, we also revealed the local reconnection mechanism of vortex lines during topology transformation. The observed evolution of isolated optical vortex topologies is strongly reminiscent of classical fluid, superfluid, and DNA recombination [3,4,48], which makes similar evolution possible in other physical fields. Thus, we believe our work should provide insight into the evolution of complex singular light fields.

Funding. National Key Research and Development Program of China (2017YFA0303800); National Natural Science Foundation of China (11634010, 11774289, 11804277, 12074312, 91850118); Basic research plan of natural science in Shaanxi province (2019JM-583, 2019JQ-616); Fundamental Research Funds for the Central Universities (3102019JC008); Innovation Foundation for Doctor Dissertation of Northwestern Polytechnical University (CX202048, CX202046).

Disclosures. The authors declare no conflicts of interest.

Data availability. Data underlying the results presented in this paper are not publicly available at this time but may be obtained from the authors upon reasonable request.

References

1. M. Berger, "Introduction to magnetic helicity," Plasma Phys. Control. Fusion **41**(12B), B167–B175 (1999).
2. D. M. Raymer and D. E. Smith, "Spontaneous knotting of an agitated string," Proc. Natl. Acad. Sci. U. S. A. **104**(42), 16432–16437 (2007).
3. D. Kleckner and W. T. M. Irvine, "Creation and dynamics of knotted vortices," Nat. Phys. **9**(4), 253–258 (2013).
4. D. Kleckner, L. H. Kauffman, and W. T. M. Irvine, "How superfluid vortex knots untie," Nat. Phys. **12**(7), 650–655 (2016).
5. F. Maucher and P. Sutcliffe, "Untangling Knots Via Reaction-Diffusion Dynamics of Vortex Strings," Phys. Rev. Lett. **116**(17), 178101 (2016).
6. J.-S. B. Tai and I. I. Smalyukh, "Three-dimensional crystals of adaptive knots," Science **365**(6460), 1449–1453 (2019).
7. T. Machon and G. P. Alexander, "Knotted Defects in Nematic Liquid Crystals," Phys. Rev. Lett. **113**(2), 027801 (2014).
8. Y. Kawaguchi, M. Nitta, and M. Ueda, "Knots in a Spinor Bose-Einstein Condensate," Phys. Rev. Lett. **100**(18), 180403 (2008).
9. D. S. Hall, M. W. Ray, K. Tiurev, E. Ruokokoski, A. H. Gheorghe, and M. Möttönen, "Tying quantum knots," Nat. Phys. **12**(5), 478–483 (2016).
10. M. S. Soskin and M. V. Vasnetsov, "Nonlinear singular optics," Pure Appl. Opt. **7**(2), 301–311 (1998).
11. M. S. Soskin and M. V. Vasnetsov, "Chapter 4 - Singular optics," in *Progress in Optics*, E. Wolf, ed. (Elsevier, 2001), pp. 219–276.
12. M. R. Dennis, K. O'Holleran, and M. J. Padgett, "Singular Optics: Optical Vortices and Polarization Singularities," in *Progress in Optics*, E. Wolf, ed. (Elsevier, 2009), pp. 293–363.
13. Y. Shen, X. Wang, Z. Xie, C. Min, X. Fu, Q. Liu, M. Gong, and X. Yuan, "Optical vortices 30 years on: OAM manipulation from topological charge to multiple singularities," Light: Sci. Appl. **8**(1), 90 (2019).
14. M. J. Padgett, "Orbital angular momentum 25 years on," Opt. Express **25**(10), 11265–11274 (2017).
15. K. O'Holleran, M. R. Dennis, and M. J. Padgett, "Topology of Light's Darkness," Phys. Rev. Lett. **102**(14), 143902 (2009).
16. M. V. Berry and M. R. Dennis, "Knotted and linked phase singularities in monochromatic waves," Proc. R. Soc. A **457**(2013), 2251–2263 (2001).
17. M. V. Berry and M. R. Dennis, "Knotting and unknotting of phase singularities: Helmholtz waves, paraxial waves and waves in 2 + 1 spacetime," J. Phys. A: Math. Gen. **34**(42), 8877–8888 (2001).
18. J. Leach, M. R. Dennis, J. Courtial, and M. J. Padgett, "Laser beams: knotted threads of darkness," Nature **432**(7014), 165 (2004).
19. M. R. Dennis, R. P. King, B. Jack, K. O'Holleran, and M. J. Padgett, "Isolated optical vortex knots," Nat. Phys. **6**(2), 118–121 (2010).
20. X. Guo, P. Li, J. Zhong, S. Liu, B. Wei, W. Zhu, S. Qi, H. Cheng, and J. Zhao, "Tying Polarization-Switchable Optical Vortex Knots and Links via Holographic All-Dielectric Metasurfaces," Laser Photonics Rev. **14**(3), 1900366 (2020).
21. L. Wang, W. Zhang, H. Yin, and X. Zhang, "Ultrasmall Optical Vortex Knots Generated by Spin-Selective Metasurface Holograms," Adv. Opt. Mater. **7**(10), 1900263 (2019).
22. A. S. Desyatnikov, D. Buccoliero, M. R. Dennis, and Y. S. Kivshar, "Spontaneous knotting of self-trapped waves," Sci. Rep. **2**(1), 771 (2012).
23. J. Zhong, S. Qi, S. Liu, P. Li, B. Wei, X. Guo, H. Cheng, and J. Zhao, "Accurate and rapid measurement of optical vortex links and knots," Opt. Lett. **44**(15), 3849–3852 (2019).
24. F. Maucher, S. Skupin, S. A. Gardiner, and I. G. Hughes, "Creating Complex Optical Longitudinal Polarization Structures," Phys. Rev. Lett. **120**(16), 163903 (2018).

Optics EXPRESS

25. H. Larocque, D. Sugic, D. Mortimer, A. J. Taylor, R. Fickler, R. W. Boyd, M. R. Dennis, and E. Karimi, "Reconstructing the topology of optical polarization knots," Nat. Phys. **14**(11), 1079–1082 (2018).
26. M. R. Dennis, "Polarization singularities in paraxial vector fields: morphology and statistics," Opt. Commun. **213**(4-6), 201–221 (2002).
27. K. Y. Bliokh, M. A. Alonso, and M. R. Dennis, "Geometric phases in 2D and 3D polarized fields: geometrical, dynamical, and topological aspects," Rep. Prog. Phys. **82**(12), 122401 (2019).
28. H. Larocque, A. D'Errico, M. F. Ferrer-Garcia, A. Carmi, E. Cohen, and E. Karimi, "Optical framed knots as information carriers," Nat. Commun. **11**(1), 5119 (2020).
29. J. A. Rodrigo, T. Alieva, E. Abramochkin, and I. Castro, "Shaping of light beams along curves in three dimensions," Opt. Express **21**(18), 20544–20555 (2013).
30. D. Sugic, M. R. Dennis, F. Nori, and K. Y. Bliokh, "Knotted polarizations and spin in three-dimensional polychromatic waves," Phys. Rev. Res. **2**(4), 042045 (2020).
31. M. F. Ferrer-Garcia, A. D'Errico, H. Larocque, A. Sit, and E. Karimi, "Polychromatic electric field knots," Phys. Rev. Res. **3**(3), 033226 (2021).
32. G. Burde and H. Zieschang, *Knots* (De Gruyter, 2008).
33. G. Gbur, "Fractional vortex Hilbert's Hotel," Optica **3**(3), 222–225 (2016).
34. M. V. Berry, "Optical vortices evolving from helicoidal integer and fractional phase steps," J. Opt. A: Pure Appl. Opt. **6**(2), 259–268 (2004).
35. H. Ma, X. Li, H. Zhang, J. Tang, H. Li, M. Tang, J. Wang, and Y. Cai, "Optical vortex shaping via a phase jump factor," Opt. Lett. **44**(6), 1379–1382 (2019).
36. J. Hu, Y. Tai, L. Zhu, Z. Long, M. Tang, H. Li, X. Li, and Y. Cai, "Optical vortex with multi-fractional orders," Appl. Phys. Lett. **116**(20), 201107 (2020).
37. J. Leach, E. Yao, and M. J. Padgett, "Observation of the vortex structure of a non-integer vortex beam," New J. Phys. **6**, 71 (2004).
38. S. N. Alperin and M. E. Siemens, "Angular Momentum of Topologically Structured Darkness," Phys. Rev. Lett. **119**(20), 203902 (2017).
39. Z. Liu, S. Yan, H. Liu, and X. Chen, "Superhigh-Resolution Recognition of Optical Vortex Modes Assisted by a Deep-Learning Method," Phys. Rev. Lett. **123**(18), 183902 (2019).
40. J. S. Birman and Braids, *Links and Mapping Class Groups* (Princeton University, 1974).
41. P. M. Sutcliffe and A. T. Winfree, "Stability of knots in excitable media," Phys. Rev. E **68**(1), 016218 (2003).
42. B. Bode, M. R. Dennis, D. Foster, and R. P. King, "Knotted fields and explicit fibrations for lemniscate knots," Proc. R. Soc. A **473**(2202), 20160829 (2017).
43. J. Leach, M. R. Dennis, J. Courtial, and M. J. Padgett, "Vortex knots in light," New J. Phys. **7**, 55 (2005).
44. R. P. King, *Knotting of optical vortices* (University of southampton, 2010).
45. F. S. Roux, "Polynomial Gaussian beams and topological charge conservation," Opt. Commun. **266**(2), 433–437 (2006).
46. F. S. Roux, "Topological charge inversion in polynomial astigmatic Gaussian beams," Opt. Commun. **281**(17), 4205–4210 (2008).
47. A. Ferrando and M. A. García-March, "Analytical solution for multi-singular vortex Gaussian beams: the mathematical theory of scattering modes," J. Opt. **18**(6), 064006 (2016).
48. K. Shimokawa, K. Ishihara, I. Grainge, D. J. Sherratt, and M. Vazquez, "FtsK-dependent XerCD-dif recombination unlinks replication catenanes in a stepwise manner," Proc. Natl. Acad. Sci. U. S. A. **110**(52), 20906–20911 (2013).